

**IMPLEMENTATION OF DSP BASED SENSORLESS CONTROL WITH  
DIRECT BACK-EMF DETECTION METHOD FOR BLDC MOTOR**

**by**

**NAGADEVEN A/L KARUNAKARAN**

**Thesis submitted in fulfillment of the  
requirements for the degree  
of Master of Science**

**FEBRUARY 2008**

## **ACKNOWLEDGEMENTS**

I am greatly indebted and respectful to my supervisor and advisor, Dr. K.S. Rama Rao, for his guidance and support throughout the completion of this thesis. His rigorous attitude to do the research and inspiring thinking to solve problems are invaluable for my professional career.

I would like to express my heartfelt thanks to Dr Soib Taib for his time and efforts he spent as my co-supervisor. I am also grateful to the faculty and staff members of Universiti Sains Malaysia, for their help.

I would like to express my appreciation to my fellow graduate students in USM. To me, the friendship with the members of USM is a big treasure. Their hardworking, perseverance, sharing, and self-motivation have always inspired me.

## **TABLE OF CONTENTS**

	Page
<b>ACKNOWLEDGEMENTS</b>	ii
<b>TABLE OF CONTENTS</b>	iii
<b>LIST OF TABLES</b>	vi
<b>LIST OF FIGURES</b>	vii
<b>LIST OF SYMBOLS</b>	xi
<b>LIST OF ABBREVIATIONS</b>	xi
<b>LIST OF APPENDICES</b>	xii
<b>LIST OF PUBLICATIONS &amp; SEMINARS</b>	xii
<b>ABSTRAK</b>	xiii
<b>ABSTRACT</b>	xiv

### **CHAPTER ONE: INTRODUCTION TO BLDC MOTOR**

1.0	Research Objective	1
1.1	Research Methodology	1
1.2	Literature Review	3
1.3	BLDC Motor Background	5
1.4	Construction and Operating Principle of BLDC Motor	8
1.4.1	Stator Construction	8
1.4.2	Rotor Construction	9
1.5	Theory of Operation of BLDC Motor	10
1.6	Torque and Speed Characteristics of BLDC Motor	11
1.7	Sensorless BLDC Motor Drives	12

### **CHAPTER TWO : DIRECT BACK EMF DETECTION FOR SENSORLESS BLDC MOTOR DRIVES**

2.0	Introduction	17
2.1	Conventional Back EMF Detection Schemes	17
2.2	Implemented Direct Back EMF Detection Scheme	23
2.3	Summary Of Proposed Direct Back EMF Detection Scheme	31

### **CHAPTER THREE: SIMULATION OF BLDC MOTOR DRIVE**

3.0	Modeling the BLDC Motor	33
3.1	Back EMF Modeling	33
3.2	BLDC Motor and Inverter Modeling	34
3.3	BLDC Main Block	39
3.4	BLDC Main Block Simulation Constants	40
3.5	The Zero Cross Block	42
3.6	The Inverter Block	45
3.7	The Changer Block	47
3.8	MATLAB Simulation Results	48

### **CHAPTER FOUR: SOFTWARE AND HARDWARE IMPLEMENTATION OF BLDC MOTOR DRIVE**

4.0	The Application Software	53
4.1	Control Algorithm of Sensorless Commutation Control	53
4.1.1	Alignment	54
4.1.2	Starting (Back-EMF Acquisition)	55
4.2	System Specification of BLDC Motor Drive	56
4.3	BLDC Motor Sensorless Drive Concept	57
4.4	The Hardware Design Overview	58
4.5	3-Phase MOSFET PWM Inverter Circuit	62
4.6	MOSFET Gate Drive Circuit	65
4.6.1	Gate Drive Scheme	66
4.6.2	MOSFET Driver Selection	67
4.6.3	MOSFET Driver Peak Current Requirement	68
4.7	dsPIC30F3010 DSP Controller Circuit	70
4.8	Overcurrent Sensing	73
4.9	Voltage Sensing	74
4.10	Zero Cross Signal Circuit	75
4.11	Internal Power Supply	76
4.12	Motor current and Fault Circuit	76
4.13	RS232 and ICD2 communication circuit	78
4.14	Speed Control Circuit	80

## **CHAPTER FIVE: RESULTS AND ANALYSIS**

5.0	Simulation and Experimental Results	81
5.1	Key Simulink BLDC Drive Simulation Waveforms	81
5.2	BLDC Motor Drive Hardware Experimental Results	86
5.3	Hardware Efficiency Measurement	93
5.3.1	Motor Output Measurements	94
5.3.2	Drive Measurements	94
5.3.3	Drive Efficiency	95
5.4	Discussion	96

## **CHAPTER SIX: CONCLUSIONS AND FUTURE RESEARCH**

6.0	Conclusions	99
6.1	Future Research	100

<b>BIBLIOGRAPHY</b>	101
---------------------	-----

## **APPENDICES**

Appendix A	Source Code of BLDC Motor Drive	104
Appendix B	M-File S-Function for delay block	129
Appendix C	MPLAB ICD2 Instruction	131
Appendix D	BLDC Motor Datasheet	146
Appendix E	Current Sense Resistor	148
Appendix F	MOSFET Driver	149
Appendix G	Power MOSFET	155
Appendix H	Power Op Amp	159
Appendix I	Comparator	161

## LIST OF TABLES

	Page
4.1 BLDC motor specifications	56
5.1 Speed versus the speed command voltage	94

## LIST OF FIGURES

	Page
1.1 Flow chart showing the research methodology.	2
1.2 Market trend for electronic motor drives in household appliances.	7
1.3 Stator of a BLDC motor.	9
1.4 Rotor magnets cross-sections.	10
1.5 Simplified BLDC motor diagrams.	11
1.6 Torque and speed characteristics of BLDC motor.	12
1.7 Structure of a BLDC motor.	12
1.8 Sensor Control of BLDC motor.	13
1.9 Sensorless control of BLDC motor.	14
1.10 Typical three phase back EMF, output torque, and phase current waveforms.	15
1.11 Winding energization based on commutation sequence.	16
2.1 Phase current and the back EMF.	18
2.2 Back EMF zero crossing detection scheme with the motor neutral point.	19
2.3 Back EMF zero crossing detection scheme with the virtual neutral point.	19
2.4 Back EMF sensing based on virtual neutral point.	21
2.5 Back EMF sensing compared to half of the dc bus.	22
2.6 Proposed back EMF zero crossing detection scheme.	24
2.7 Proposed PWM strategy for direct back EMF detection scheme.	25
2.8 Circuit model of motor and power inverter drive topology.	26
2.9 Circuit model of proposed back EMF detection during the PWM off time moment at terminal C.	29
3.1 Trapezoidal back EMF pattern.	34
3.2 Schematic diagram of the simulation circuit.	38
3.3 Simulink BLDC motor block.	39

3.4	Simulink BLDC motor simulation constant block.	41
3.5	Printout of the BLDC S-function block.	42
3.6	Zero cross block outline diagram.	43
3.7	Construction diagram of simulink zero cross block.	44
3.8	Structure of power inverter.	45
3.9	Simulink BLDC motor inverter block.	46
3.10	Simulink changer block.	47
3.11	Simulation waveform of 3-phase currents.	48
3.12	Simulation waveform of three phase back EMFs.	49
3.13	Terminal voltages of three phase back EMFs.	49
3.14	Terminal voltage and phase current waveforms - comparison.	50
3.15	Simulation waveform of motor speed at low speed (500 rpm).	51
3.16	Simulation waveform of motor speed at high speed (1500 rpm).	51
3.17	Simulation waveform of torque of the BLDC motor drive.	52
4.1	Commutation control states.	54
4.2	BLDC motor drive sensorless system concept.	57
4.3	Hardware prototype of the BLDC motor sensorless drive.	58
4.4	Hardware layout of the BLDC motor sensorless drive.	59
4.5	Block diagram of the BLDC motor sensorless drive.	60
4.6	3-phase bipolar inverter outline.	62
4.7	3-phase bipolar inverter circuit on prototype hardware board.	63
4.8	MOSFET gate driver circuit on prototype hardware board.	65
4.9	Example of a high side (Q1) and low side (Q2) gate drive.	66
4.10	dsPIC30F3010 pin connection diagram.	72
4.11	dsPIC30F3010 controller circuit on prototype hardware board	73
4.12	Sense resistor circuit on prototype hardware board.	74
4.13	Voltage divider circuit on prototype hardware board.	74



4.14	Zero crossing circuit on prototype hardware board.	75
4.15	Internal power supply circuit on prototype hardware board.	76
4.16	Motor current monitoring circuit on prototype hardware board.	77
4.17	Fault monitoring circuit on prototype hardware board.	78
4.18	RS232 and ICD2 communication circuit on prototype hardware board.	79
4.19	Speed control circuit on prototype hardware board.	80
5.1	Simulation waveform of 3-phase current.	81
5.2	Simulation waveform of three phase back EMF.	82
5.3	Simulation waveform of terminal voltage.	82
5.4	Comparison of simulation waveform of each phase of BEMF and each phase of terminal voltage.	83
5.5	Comparison of simulation waveform of each phase of BEMF and each phase of current.	84
5.6	Simulation waveform of motor speed at low speed (500 rpm).	85
5.7	Simulation waveform of motor speed at high speed (1500 rpm).	85
5.8	Simulation waveform of torque of the simulated BLDC motor drive.	86
5.9	24 V regulated voltage waveform.	87
5.10	15 V regulated voltage waveform.	87
5.11	5 V regulated voltage waveform.	87
5.12	PWM driving pulses for $Q_{A+}$ and $Q_{A-}$ .	88
5.13	PWM driving pulses for $Q_{B+}$ and $Q_{B-}$ .	88
5.14	PWM driving pulses for $Q_{C+}$ and $Q_{C-}$ .	89
5.15	PWM driving pulses for $Q_{A+}$ , $Q_{A-}$ , $Q_{B+}$ , $Q_{B-}$ , $Q_{C+}$ and $Q_{C-}$ .	89
5.16	Back EMF waveforms comparison for phase A and phase B.	90
5.17	Back EMF waveforms comparison for phase B and phase C.	90
5.18	Back EMF waveforms comparison for phase C and phase A.	91

5.19	Back EMF waveforms comparison for phase A, phase B and phase C.	91
5.20	Phase current waveforms comparison for phase A, phase B and phase C.	92
5.21	Power measurement diagram on BLDC motor drive system.	93
5.22	Sequence of zero crossing of back EMF and phase commutation.	97

## LIST OF SYMBOLS

1.1	$\omega$ - Rotor Speed	31
1.2	$\theta$ - Rotor Position	31
1.3	$\lambda$ - Flux Linkage	31
1.4	$\Omega$ - Ohm (Resistance)	25
1.5	$f$ - Frequency, Hz	60

## LIST OF ABBREVIATIONS

1.1	BLDC - Brushless direct current	1
1.2	EMF – Electromotive force	1
1.3	DSP – Digital signal processor	1
1.4	ASD - Adjustable speed drives	6
1.5	EMD - Electronic motor drives	6
1.6	AC – Alternating current	7
1.7	TP – Peak torque	11
1.8	TR – Rated torque	11
1.9	RPM – Rotation per minute	14
1.10	PWM – Pulse width modulation	19
1.11	IDE – Integrated development environment	55
1.12	ADC – Analog to digital converter	55

## **LIST OF APPENDICES**

1.1	Appendix A	Source Code of BLDC Motor Drive	104
1.2	Appendix B	M-File S-Function for delay block	129
1.3	Appendix C	MPLAB ICD2 Instruction	131
1.4	Appendix D	BLDC Motor Datasheet	146
1.5	Appendix E	Current Sense Resistor	148
1.6	Appendix F	MOSFET Driver	149
1.7	Appendix G	Power MOSFET	155
1.8	Appendix H	Power Op Amp	159
1.9	Appendix I	Comparator	161

## **LIST OF PUBLICATIONS & SEMINARS**

	Page
1.1 International Conference on Robotics, Vision, Information & Signal Processing (ROVISP 2005).	164
1.2 The 1st International Conference on Control, Instrumentation and Mechatronics (CIM '07).	170

# **IMPLEMENTASI KAWALAN TANPA SENSOR BERASASKAN DSP DENGAN KAEDAH PENGESANAN EMF BALIK SECARA TERUS UNTUK MOTOR BLDC**

## **ABSTRAK**

Projek ini mempersembahkan satu kaedah baru untuk mengesan voltan balikkan EMF tanpa sensor untuk sistem pacuan BLDC dengan mengaplikasikan kawalan digital DSP (digital signal processor). Dengan kaedah ini voltan neutral motor tidak diperlukan untuk mengesan EMF balik. Sebaliknya, kaedah ini menggunakan rangkaian A/D berkelajuan tinggi yang terdapat pada pengawal DSP. EMF balikan yang sebenar bagi lingkaran motor yang terapung dapat dikesan ketika masa tutup PWM kerana voltan terminal bagi motor adalah bertindak secara terus dengan fasa EMF balik pada ketika ini. Voltan EMF balik juga dirujukkan pada sambungan bumi tanpa sebarang kesan hingar. Dengan itu, kaedah pengesanan EMF balik ini tidak dipengaruhi oleh hangar pensuisan PWM. Justeru itu, peningkatan dan penapisan isyarat tidak diperlukan.

Simulasi untuk projek ini telah diimplementasi dengan menggunakan perisian Simulink Matlab. Dalam simulasi, elemen utama seperti kelajuan, 'torque', arus fasa, voltan terminal, dan voltan EMF balik diperhati. Model simulasi untuk motor BLDC, marangkumi penyelesaian menggunakan keadah pengamiran bergantung kepada input kepada motor dan konstan simulasi. Model matematik bagi system pacuan telah dibina untuk menganalisis keupayaan system pacuan yang direkebentuk.

Sistem pacuan ini menggunakan sistem digital DSP, yang telah diprogramkan dengan program kawalan tanpa sensor untuk system pacuan motor BLDC. Implementasi melalui bahasa program DSP telah megurangkan bilangan komponen dan mempercepatkan respon dari pengawal. DSP berpretasi tinggi yang digunakan telah mengurangkan masa lingkaran kawalan. Pengubahsuaian dapat dilakukan dengan mudah pada struktur kawalan dengan memprogram perisian baru ke dalam

pengawal. Kesahihan system pacuan yang direkabentuk telah diperiksa melalui keputusan ujian kaedah simulasi dan pembinaan prototaip. Prototaip yang dibina mempunyai julat operasi pada 24V, 5A. Berdasarkan analisis yang dijalankan keputusan prototaip menyamai keputusan simulasi.

# **IMPLEMENTATION OF DSP BASED SENSORLESS CONTROL WITH DIRECT BACK-EMF DETECTION METHOD FOR BLDC MOTOR**

## **ABSTRACT**

This thesis presents a back EMF sensing scheme, direct back EMF detection, for sensorless Brushless DC (BLDC) motor drives with a DSP based controller. Using this scheme, the motor neutral voltage is not needed to measure the back EMF. Instead the method utilizes the high-speed A/D converter channels, which are available on a DSP controller. The true back EMF of the floating motor winding is detected during the off time of PWM because the terminal voltage of the motor is directly proportional to the phase back EMF during this interval. Also, the back EMF voltage is referenced to ground without any common mode noise. Therefore, the developed back EMF sensing method is immune to switching noise and common mode voltage. As a result, attenuation and filtering is not necessary for the back EMF sensing.

The simulation of the BLDC motor drive system is implemented in SIMULINK MATLAB software. The simulation of the system for important characteristics such as speed, torque, phase current, terminal voltage, and Back EMF (BEMF) are monitored. The simulation modeling involves solving many simultaneous differential equations, each depending upon the inputs to the motor and the simulation constants. A mathematical model of the drive system is also developed to analyze the performance of the proposed driver.

The system is implemented developing the hardware, using a digital signal processor (dsPIC30F), which is programmed with sensorless control for BLDC motor. The implementation through assembly language programming of DSP has resulted in reduced hardware and fast response of the controller. The high performance of digital signal processors (DSPs) minimizes the control loop delays. Also further modifications

in control structure are easily possible by changing the software. The implemented hardware can support speed range up to 3500 rpm of the BLDC motor, with reduced back EMF noise. The validity of the proposed BLDC motor drive system is verified through simulation and hardware results such as phase current, back EMF signal waveforms and speed. The experimental results on a 3-phase, 24 V, 120 W BLDC motor using dsPIC30F (DSP) based digital controller closely agree with the simulation results.



# **CHAPTER I**

## **INTRODUCTION TO BRUSHLESS DIRECT CURRENT (BLDC) MOTOR**

### **1.0 Research Objective**

The objective of this thesis is to present the design of a 3-phase sensorless brushless dc (BLDC) motor control with back-EMF (electromotive force) zero-crossing sensing using an AD converter. It is based on Microchip dsPIC30F3010 DSP which is dedicated for motor control applications. The system is designed as a motor drive system for 3-phase BLDC motors and is targeted for applications in both industrial and appliance fields. The reference design incorporates both hardware and software parts of the system including details of hardware layout. This thesis also includes the basic motor theory, simulation implementation concept, hardware implementation and software design.

### **1.1 Research Methodology**

The research methodology of this thesis involves a number of different tasks that are needed to lead towards completion. The first task is to define the objective of the research in which the target specification of end product is defined. This followed by the literature review where all the theoretical information regarding the research is gathered and a comparison of previous similar research is discussed. A brief description on the BLDC motor theory and performance is then presented. The advantage of the proposed back-EMF detection scheme for sensor-less control is compared with the conventional back-EMF detection schemes. Next in this thesis, the simulation of the targeted controller implementation for the drive system using MATLAB SIMULINK software tools is discussed. The simulation waveforms of voltages, phase currents and speed response are obtained to compare with the results from proto-type hardware drive system. The next task is to design the hardware for the target controller, based on the application target. The component

ratings and type were selected. Once the hardware design is completed the software implementation is carried out. The software code matching the hardware design is developed in this stage. The next step is to integrate the software code and the hardware to debug any failures. This task is implemented with ICD2 [15] debugging software. The following task is to analyze the test results obtained with the controller and motor to determine the performance, and also the waveforms of critical parameters captured during this stage. The final stage is to conclude the research findings and the thesis write up. Figure 1.1 shows the flow chart of the research methodology of this thesis.

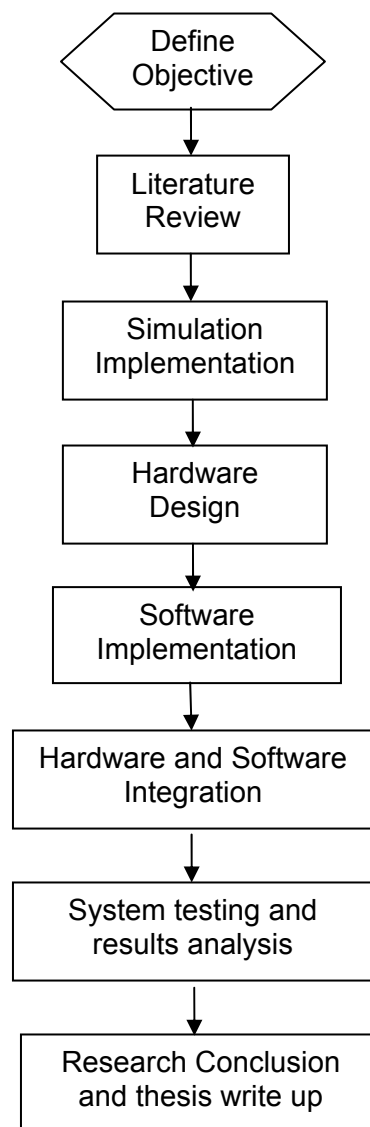


Figure1.1: Flow chart showing the research methodology.

## 1.2 Literature Review

The 3-phase BLDC motors are well adoptable for industrial applications that require medium and very high speeds. Two important characteristics, low inertia and high peak torque, result in the motor capable of quick accelerations and decelerations. Sensor and sensorless control are two methods of control of BLDC motors [1-5]. In sensor control Hall sensors are normally used which need maintenance. An approach to position sensorless BLDC motor drive [6], a new algorithm for sensorless operation [7] and sensorless control without signal injection [8] are reported. Two types of sensorless control techniques of PM BLDC motors are discussed [12]. The first type is the position sensing using back EMF of the motor, and the second one is position estimation using motor parameters. The position estimation scheme usually needs complicated computation, and the cost of the system is relatively high. The back EMF sensing scheme is the most commonly used method, which is adopted in this thesis. The advantages of the position sensing using back EMF are:

- It is suitable to be used on a wide range of motors and the method is easily implemented on both Y and  $\Delta$  connected 3-phase motors.
- It requires no detailed knowledge of motor properties.
- It is relatively insensitive to motor manufacturing tolerance variations.
- It will work for either voltage or current control.

In a 3-phase BLDC motor, only two out of three phases are excited at any time, leaving the third phase winding floating. The back EMF voltage in the floating winding can be measured to establish a switching sequence for commutation of power devices in the 3-phase inverter. The conventional method of sensing back EMF is to build a virtual neutral point that will, in theory, be at the same potential as the center of a Y wound motor and then to sense the difference between the virtual neutral and the voltage at the floating

terminal. However, when using a chopping drive, the neutral is not a standstill point. The neutral potential jumps from zero up to near dc bus voltage, creating a large common mode voltage since the neutral is the reference point [9].

Meanwhile, the PWM signal is superimposed on the neutral voltage as well, inducing a large amount of electrical noise on the sensed signal. Proper sensing of the back EMF requires a lot of attenuation and filtering. The attenuation is required to bring the signal down to the allowable common mode range of the sensing circuit, and the low pass filtering is to smooth the high switching frequency noise. The result is a poor signal to noise ratio of a very small signal, especially at start-up where it is needed most. Consequently, this method tends to have a narrow speed range and poor start up characteristics. To reduce the switching noise, the back EMF integration [13], third harmonic voltage integration [10] and flux estimation [7] were introduced.

The integration approach has the advantage of reduced switching noise sensitivity. However, it still has the problem of high common mode voltage in the neutral. The flux estimation method has estimation error at low speeds. An indirect sensing of zero crossing of phase back EMF by detecting conducting state of free-wheeling diodes in the unexcited phase was also approached [6]. The implementation of this method is complicated and costly, while its low speed operation is still a problem.

In this thesis a back EMF detection method, which does not require the motor neutral voltage is implemented. The back EMF can be detected directly from the terminal voltage by properly choosing the PWM and sensing strategy. The resulting feedback signal is not attenuated, providing a signal with a very good signal/noise ratio. As a result the

proposed sensorless BLDC motor drive provides a much wider speed range up to 4000 rpm, from start-up to full speed, than the conventional approaches mentioned above.

The report of this thesis conducts the theoretical analysis of the concept of the direct back EMF detection scheme, providing detailed understanding of the method. In the past, several integrated circuits based on neutral voltage construction have been commercialized [16, 17]. Unfortunately, all these ICs are all analog devices, which lack flexibility in applications, regardless of poor performance at low speed. Use of 8-bit microcontrollers have been the mainstay of embedded-control systems for a long time [9]. However, the computational power and command execution speed of these controllers is lower compared to a Digital Signal Processor (DSP).

One single-chip architectural platform that is ideal for BLDC motor control is the 16-bit Digital Signal Controller (DSC). The DSPs can apply very complicated control theory and speed estimation for the sensorless BLDC motor control. The DSP devices are available for a low cost; and the instructions sets are easy to use. Low system cost and high flexibility are good motivations to design a new DSP based controller which is dedicated to sensorless BLDC drive [18]. The flexibility mentioned here are the further modifications in control structure easily accomplished by changing the software programming. As a result, a low cost DSP based controller is developed, implementing the proposed back EMF sensing scheme.

### **1.3 Brushless Direct Current (BLDC) Motor Background**

Brushless Direct Current (BLDC) motors are one of the motor types which currently becoming popular. BLDC motors are utilized in wide range of industries such as consumer electronics, medical, automotive, industrial automation equipment and aerospace. The

commutation of BLDC motors are not the same as the brush type DC motor. The mechanical commutator of the brush dc motor is replaced by electronic switches, which supply current to the motor windings as a function of the rotor position. This kind of ac motor is called a brushless dc motor, since its performance is similar to the traditional dc motor with commutators. BLDC motors have many advantages compared to brush type DC motors and induction motors, listed as follows [1-5]:

- Better speed versus torque characteristics.
- High dynamic response.
- High efficiency.
- Long operating life.
- Noiseless operation.
- Higher speed ranges.

In addition, the ratio of torque delivered to the size of the motor is higher, making it useful in applications where space and weight are critical factors. Over the years of advanced technology development in power semiconductors, embedded systems, adjustable speed drives (ASDs) control schemes and permanent-magnet brushless electric motor production have contributed for reliable and cost-effective solution for adjustable speed applications. Household appliances are expected to be one of fastest-growing end product market for electronic motor drives (EMDs) over the following next few years [19]. The major appliances include clothes washers, room air-conditioners, refrigerators, vacuum cleaners, freezers, etc. The market volume is predicted to be a 26% compound annual growth rate over the five years from 2000 to 2005, as shown in Figure 1.2.

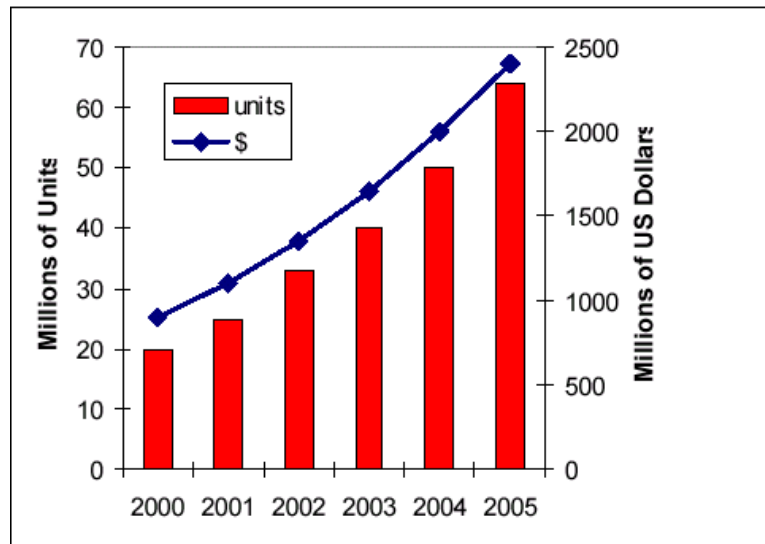


Figure1.2: Market trend for electronic motor drives in household appliances [19].

The automotive industry will also see the explosive growth ahead for BLDC type electronically controlled motor system owing to the compact design and high efficiency of BLDC motor. The appliances and devices use the electric motors to convert electrical energy into useful mechanical energy required by the load. Consumers now demand for lower energy costs, better performance, reduced acoustic noise, and more convenience features. In recent years, proposals have been made for new higher energy-efficiency standards for appliance industry, which will be legalized in near future [20]. These energy standards proposals present new challenges for appliance designers. The continuous global demand for higher efficiency and better performance, enable the transition of industries to switch over to ASDs. The BLDC motor drive system which is cost effective with high performance will be the sought after system.

## **1.4 Construction and Operating Principal of BLDC Motor**

BLDC motors can be classified as a kind of synchronous motor. Generally for synchronous motor the magnetic field generated by the stator and the magnetic field generated by the rotor rotate at the same frequency. BLDC motors can be classified as single-phase, 2-phase and 3-phase configurations. As the name indicates, the stator has the corresponding number of windings. Out of these, 3-phase motors are the most popular and widely used, which is the topic in this thesis.

### **1.4.1 Stator Construction**

BLDC motors have three stator windings connected in star or delta pattern. Most of the available BLDC motors have star type winding connection. Each of these windings are constructed with numerous coils interconnected to form a winding. One or more coils are placed in the slots and they are interconnected to make a winding. Each of these windings is distributed over the stator periphery to form an even numbers of poles [1-5]. The stator windings are designed either distributed or concentrated types, each generating sinusoidal or trapezoidal types of back electromotive force (BEMF) respectively. The phase current also has trapezoidal or sinusoidal variations. This thesis deals with the concentrated type stator windings construction. The stator of a BLDC motor consists of stacked steel laminations with windings placed in the slots that are axially cut along the inner periphery, as shown in Figure 1.3.





Figure1.3: Stator of a BLDC motor [13].

#### 1.4.2 Rotor Construction

The construction of BLDC motor rotor is made of permanent magnet materials. The pole pairs can vary from two to eight pole pairs with alternate North (N) and South (S) poles. The proper magnetic material to create the rotor is selected based upon the required magnetic-field density. Traditionally ferrite magnets are used to make permanent magnets, but recently as the technology advanced, rare earth alloy magnets are gaining popularity. The disadvantage of the ferrite magnets is having low flux density for a given volume even though it is cheaper compared to rare earth alloy magnets. In contrast, the rare earth alloy material has a high magnetic density per volume and enables the reduction of rotor size for the same applied torque. Another advantage of these alloy magnets are the improvement of size-to-weight ratio and provide higher torque for the same size motor using ferrite magnets. The type of rare earth alloy magnets that recently gaining popularity are such as Neodymium (Nd), Samarium Cobalt (SmCo) and the alloy of Neodymium, Ferrite and Boron (NdFeB). Continuous research is going on to improve the flux density to

compress the rotor further [1-5]. Figure 1.4 shows the cross sections of different arrangements of magnets in a rotor.

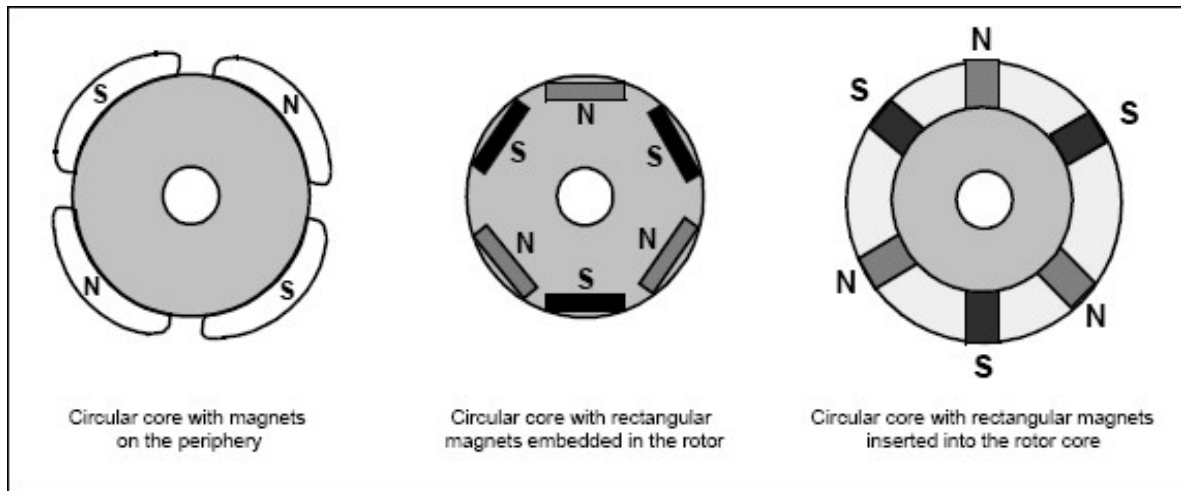


Figure1.4: Rotor magnet cross-sections [13].

## 1.5 Theory of Operation of BLDC Motor

The commutation sequence for BLDC motors has one of the windings energized to positive power (current enters into the winding), the second winding is negative (current exits the winding) and the third is in a non-energized condition. The interaction between the magnetic field generated by the stator coils and the permanent magnets creates the required torque. Ideally, the peak torque occurs when these two fields are at  $90^\circ$  to each other. In order to keep the motor running, the magnetic field produced by the windings should shift position, as the rotor moves to catch up with the stator field. The motor construction with star connection consists of three electromagnetic circuits connected at a common point, also referred to as neutral point. Each electromagnetic circuit is split in the center, thereby permitting the permanent magnet rotor to move in the middle of the induced magnetic field. The key to electronic commutation is to sense the rotor position, and then energize the correct winding phases to keep the rotor rotating. Figure 1.5 is a

simplified illustration of the motor construction with its winding topology and star connection.

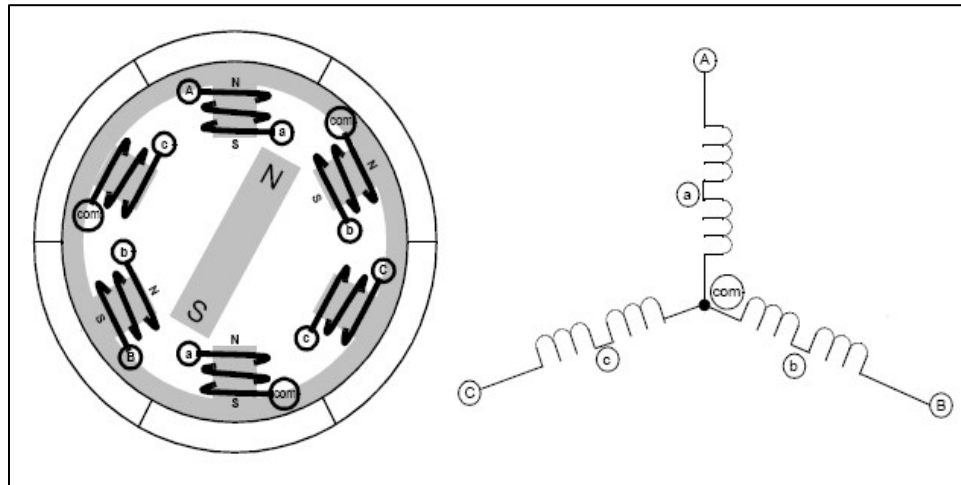


Figure1.5: Simplified BLDC motor diagrams [13].

## 1.6 Torque and Speed Characteristic of BLDC Motor

There are two torque parameters used to define a BLDC motor, peak torque ( $T_P$ ) and rated torque ( $T_R$ ). During the operations, the motor can be loaded up to the rated torque where the torque remains constant for a speed range up to the rated speed. The motor can be run up to the maximum speed, which is up to 150 % of the rated speed, but the torque starts dropping [13]. Some applications demand more torque than the rated torque especially when the motor starts from a standstill and during acceleration. During this period, extra torque is required to overcome the inertia of the load and the rotor itself. The BLDC motor can deliver the extra-required torque, maximum up to peak torque, as long as it is operated within the zone of the speed torque curve. Figure 1.6 shows an example of torque and speed characteristics of BLDC motor.

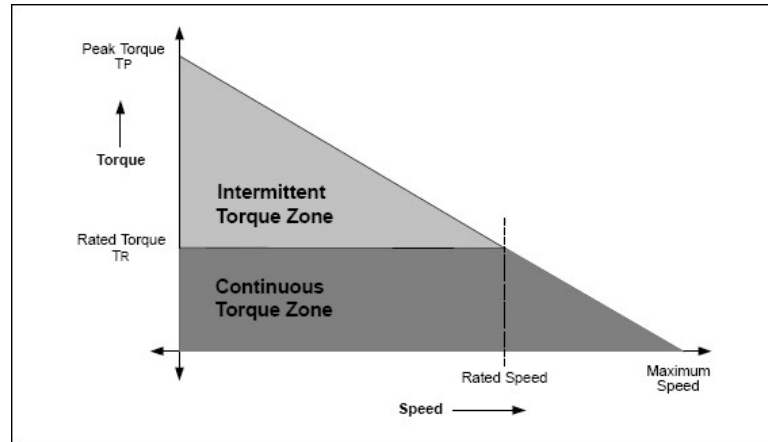


Figure 1.6: Torque and speed characteristics of BLDC motor [13].

## 1.7 Sensorless BLDC Motor Drives

The BLDC motor drive system consists of a dc power supply switched to the stator phase windings of the motor through an inverter by power switching devices. The detection of rotor position will determine the switching sequence of the inverter. The phase current of the motor, in typically rectangular shape, is synchronized with the back EMF to produce constant torque at a constant speed. Three-phase inverters are generally used to control these motors, requiring a rotor position sensor for starting and for providing the proper commutation sequence to stator windings. These position sensors can be Hall sensors, resolvers, or absolute position sensors. Figure 1.7 shows the structure of a BLDC motor.

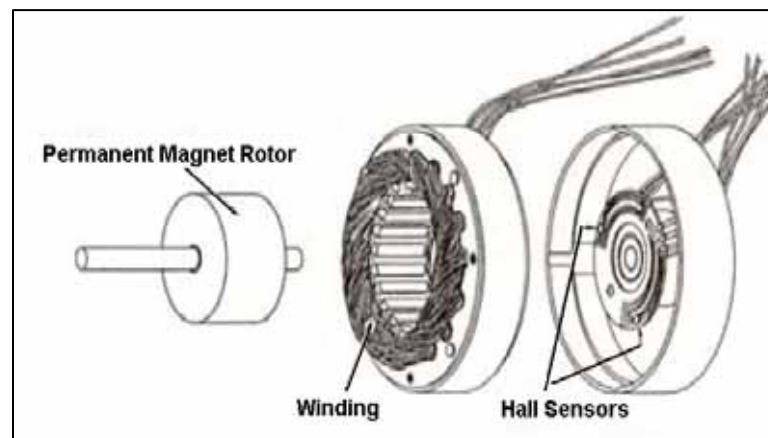


Figure1.7: Structure of a BLDC motor [15].

The disadvantages of sensed motor control system are increased cost and size of the motor, and need special mechanical arrangement for mounting the sensors. A BLDC motor control system with position sensors is shown in Figure 1.8.

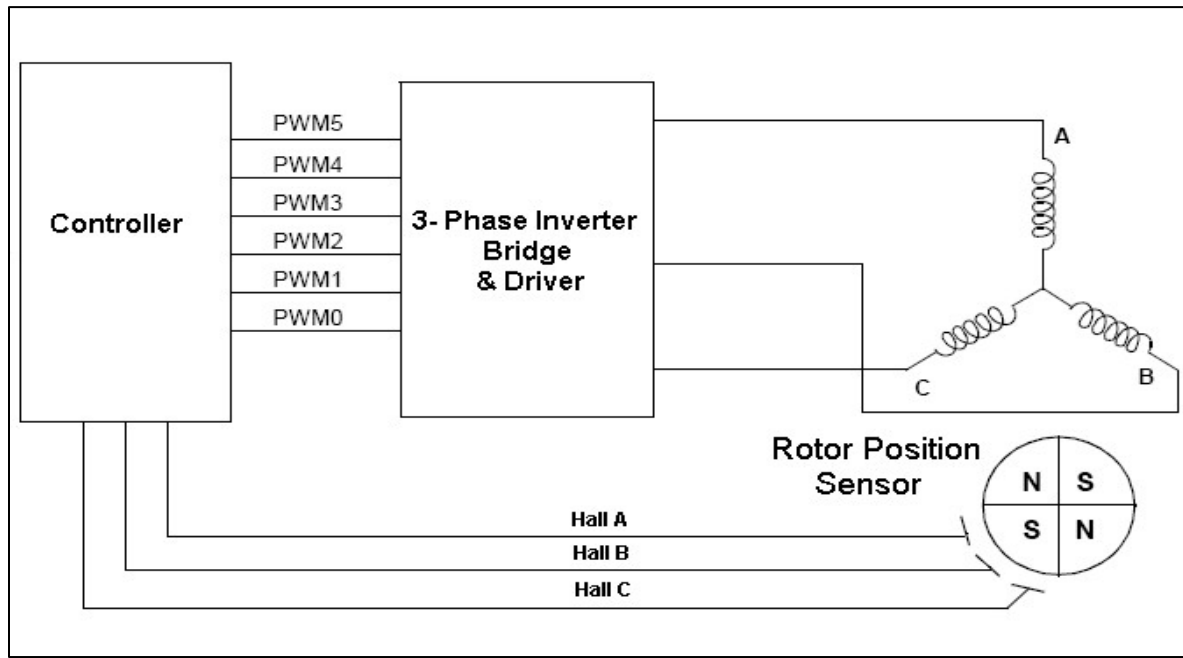


Figure1.8: Typical brushless DC motor control system with rotor position.

These position sensors, particularly Hall sensors, are temperature sensitive, limiting the operation of the motor to below about 75 °C [5]. On the other hand, they could reduce the system reliability because of the components and wiring. In some applications, it even may not be possible to mount any position sensor on the motor. Therefore, sensorless control of BLDC motor has been receiving great interest in recent years. Figure 1.9 shows the structure of sensorless control of BLDC motor.

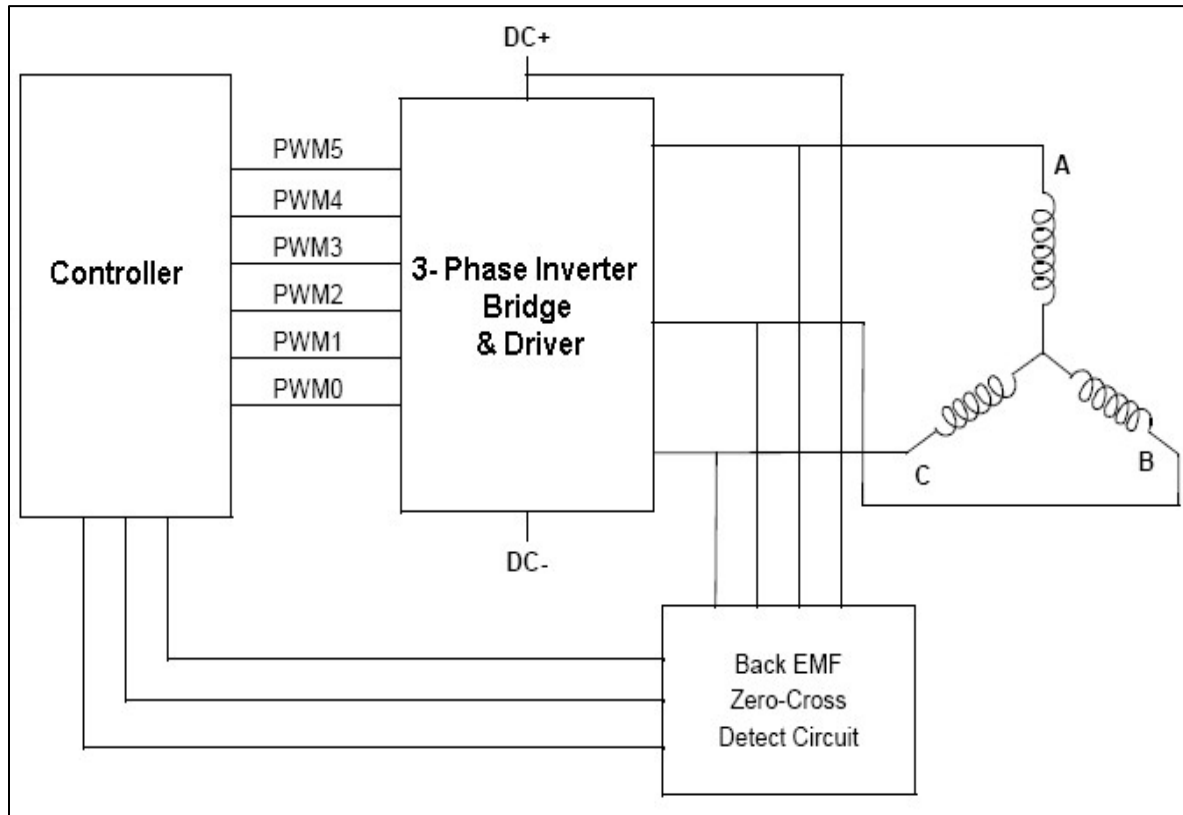


Figure1.9: Sensorless control of BLDC motor.

Sensorless method of commutation will eliminate all the Hall sensor accessories such as, sensor magnet, sensor wires, and the sensor PCB board. This will simplify the BLDC motor construction thus reducing cost. In certain applications where the motor operates in dusty environment, or generates heat will increase the Hall sensor failure. Therefore sensorless drive system is a best way to increase the overall reliability of a drive system since, the system with fewer components are more reliable. Figure 1.10 shows typical 3-phase back EMF, output torque, and phase current waveforms of the motor.

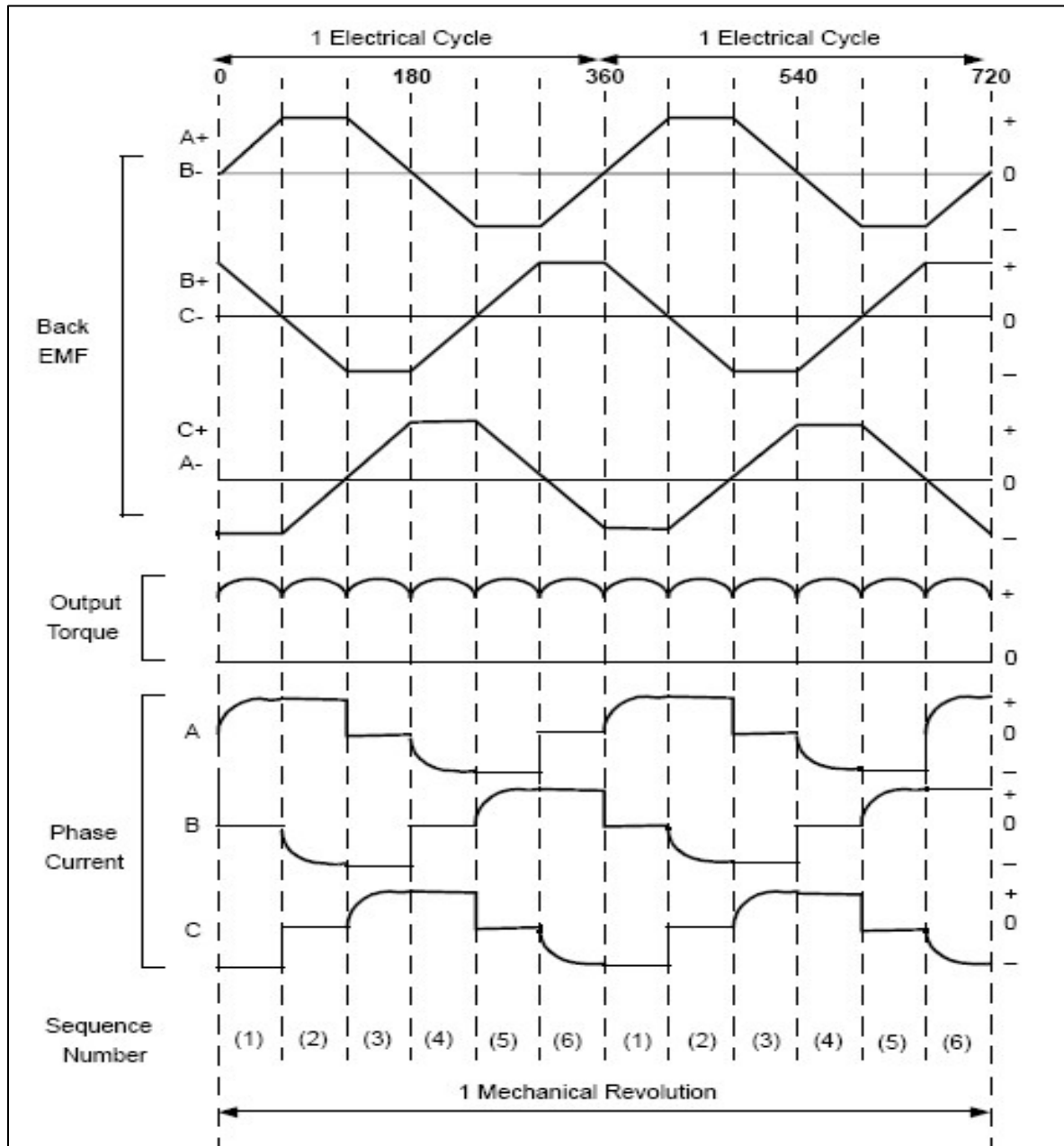


Figure 1.10: Typical three phase back EMF, output torque, and phase current waveforms [13].

Figure 1.11 shows the current flow sequence that should be followed, based on commutation sequence. The sequence numbers on Figure 1.10 correspond to the numbers given in Figure 1.11.

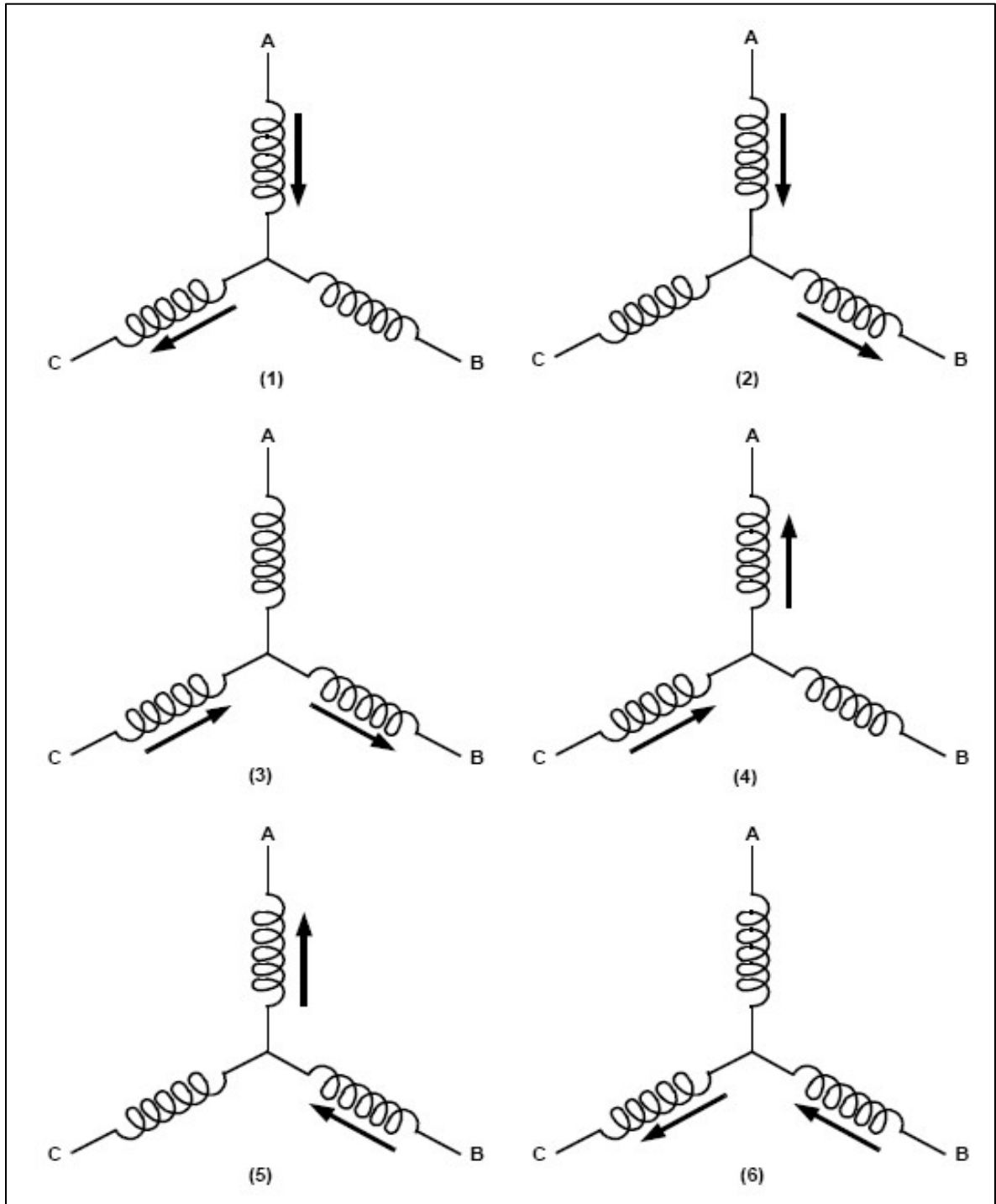


Figure1.11: Winding energization based on commutation sequence [14].



## **CHAPTER 2**

### **DIRECT BACK EMF DETECTION FOR SENSORLESS BLDC DRIVES**

#### **2.0 Introduction**

This chapter presents a brief description of the conventional virtual neutral point back EMF detection method. Then, the implemented back EMF detection scheme is discussed. In order to explain and simulate the idea of the back EMF sensing scheme and the sensorless system a simplified mathematical model based on the basic circuit topology has been described.

#### **2.1 Conventional Back EMF Detection Schemes**

A BLDC motor driven by a three-phase inverter is commonly known as, six-step commutation. The conducting interval of each phase A, B or C is  $120^\circ$  by electrical angle. The commutation follows certain pattern in one cycle; the first step is AB, then to AC, to BC, to BA, to CA, to CB and then just repeats this pattern. The conducting interval lasts for 60 electrical degrees, which is called one step, so totally, there are 6 steps in one cycle. A transition from one step to another step is called commutation. Therefore, only two phases conduct current at any time, leaving the third phase floating. For example, when phase A and phase B conduct current, then phase C is floating. In order to produce maximum torque, the inverter should be commutated every  $60^\circ$  so that current is in phase with the back EMF. The current is commutated in such a way that the current is in phase with the phase back EMF to get the optimal control and maximum torque/ampere.

The commutation timing for sensorless drive can be achieved from the back EMF on the floating windings of the motor. The back EMF on the unconnected winding is a direct indication of the rotor position and it is possible to determine the commutation timing

if the back EMF is known. If the zero crossing of the phase back EMF is detected, then the commutation of the appropriate stator windings can be implemented. Since only two phases are conducting current at one time instant, and the third winding is open, this feature enables the back EMF detection in the floating winding [21]. In Figure 2.1, the phase current is in phase with the phase back EMF.

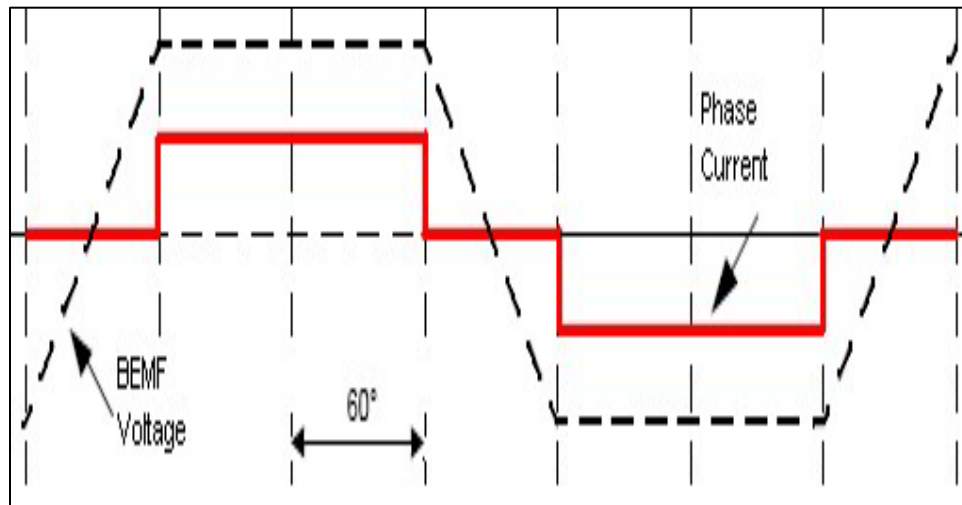


Figure2.1: Phase current and the back EMF.

The conventional back EMF zero crossing detection scheme needs the motor neutral point voltage to get the zero crossing of the back EMF, since the back EMF voltage is referred to the motor neutral point. When terminal voltage is compared to the neutral point, the zero crossing of the back EMF can be obtained. The conventional back EMF zero crossing detection scheme with the motor neutral point available is shown in Figure 2.2.

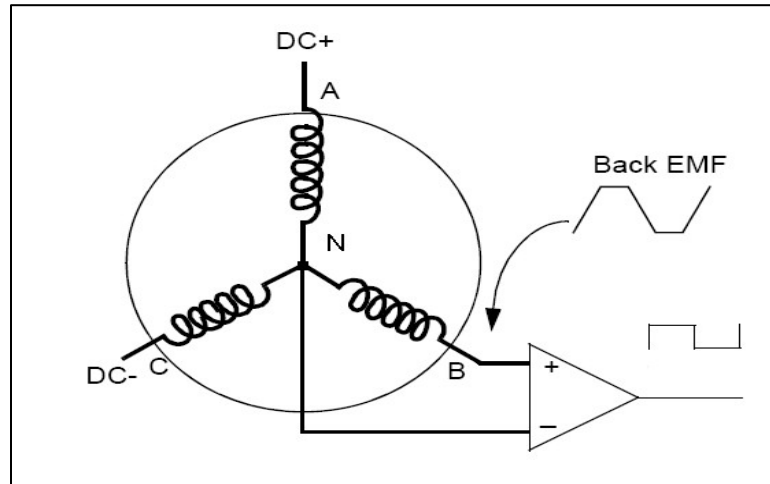


Figure2.2: Back EMF zero crossing detection scheme with the motor neutral point [6].

The motor neutral point is not available in most of the motors. In order to sense the back EMF, the most-commonly used method is to build a virtual neutral point. Theoretically this method creates a neutral point that will be at the same potential as the center of a Y wound motor. The differences between the virtual neutral and the voltage at the floating terminal are sensed to provide commutation. The virtual neutral point is built by resistors, as shown in Figure 2.3.

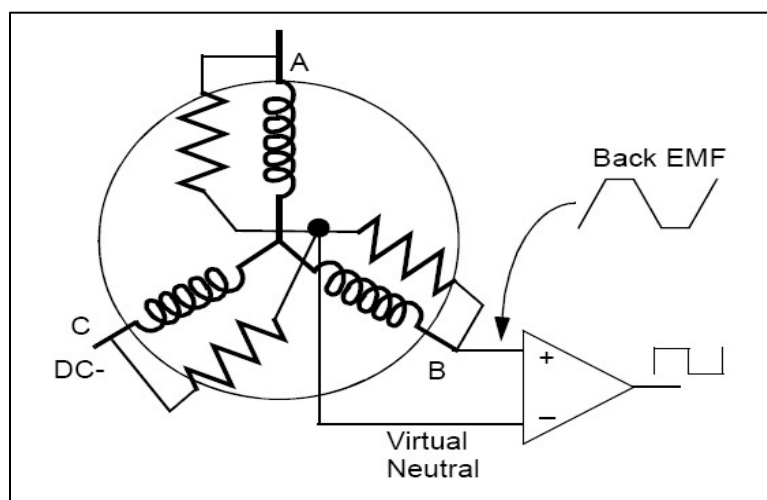


Figure2.3: Back EMF zero crossing detection scheme with the virtual neutral point [6].

The comparators output makes a transition from low to high, when the back EMF developed in the windings crosses the zero point towards positive side. When the back EMF developed in the windings crosses the zero point towards negative side the comparators output makes a transition from high to low. By having three such comparator circuits, one on each of the phases gives three digital signals corresponding to the back EMF signal in the windings. The combination of these three signals is used to derive the commutation sequence. This scheme is quite simple and has been used for a long time since the invention [11, 22]. However, this scheme has its drawbacks.

Because of the PWM drive, the neutral point is not a standstill point. The potential of this point jumps up and down. It generates very high common mode voltage and high frequency noise. Normally voltage dividers and low pass filters are used to reduce the common mode voltage and smooth the high frequency noise. For instance, if the dc bus voltage is 50 V, the potential of the neutral point may vary from zero to 50 V. The allowable common mode voltage for a comparator is typically a few volts, i.e. 5 V. The signal need to be heavily attenuated and the voltage divider will reduce the signal sensitivity at low speed, especially at start-up where it is needed most [9]. Figure 2.4, shows the back EMF sensing based on virtual neutral point.

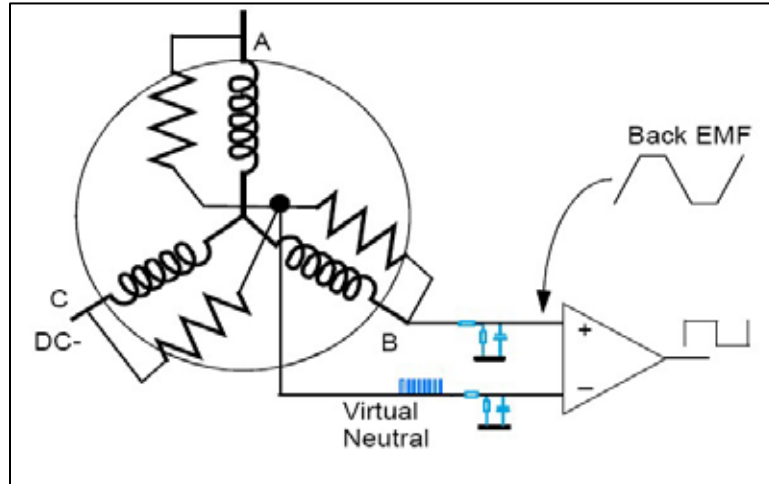


Figure2.4: Back EMF sensing based on virtual neutral point [9].

Another method of back EMF zero cross sensing is comparing the back EMF voltage to the half of the dc bus voltage by using comparators. In this method shown in Figure 2.5, phase A is connected to the positive side of the power supply (DC+), phase C is connected to the negative side of the power supply (DC-) and phase B is open. The back EMF observed in phase B increases and decreases as the power supply (DC+, DC-) are connected and disconnected to the winding terminals in the energizing sequence. By comparing the back EMF voltage and half of the dc bus, the voltage between the central point of phases A and C is obtained. Each phase requires a circuit as shown in Figure 2.5, the combination of these three signals is used to derive the commutation sequence. This scheme is easy to implement with three op-amp comparators.

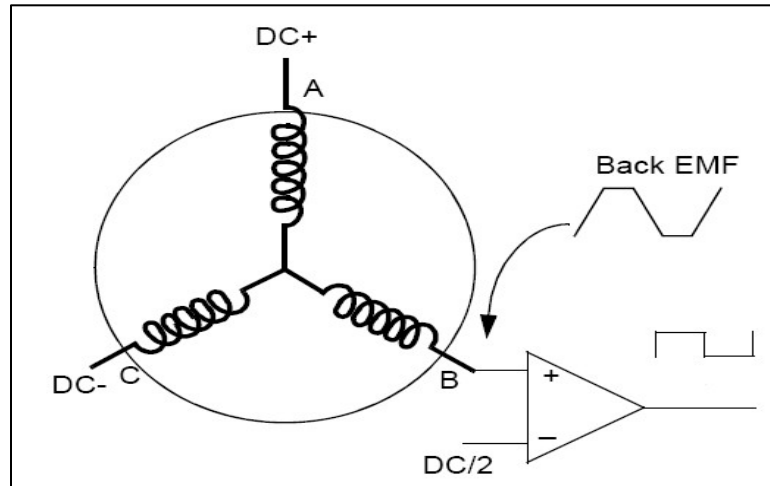


Figure2.5: Back EMF sensing compared to half of the dc bus [6].

There are few drawbacks to this circuit. First, if all three windings do not have identical characteristics, the back EMF measured will have either negative or positive phase shift. This may result in energizing the windings at different instances than they should be, and motor winding drawing excess current. Another drawback is that if the motor rated voltage is much less than the DC bus voltage, there could be a large difference between the back EMF zero cross point and half of the dc bus voltage. This could also result in having a phase shift in either direction.

A few other schemes for sensorless BLDC motor control were also developed, such as the back EMF integration, third harmonic voltage detection, and free-wheeling diodes conducting states. The back EMF integration approach has the advantage of reduced switching noise sensitivity and automatic adjustment of the inverter switching instants to changes in the rotor speed [13]. The back EMF integration method still has accuracy problems at low speeds. The rotor position is determined based on the stator third harmonic voltage component [10], in this scheme. The main disadvantage is its relatively low value of the third harmonic voltage at low speed. The rotor position

information is determined based on the conducting state of freewheeling diodes in the unexcited phase [6]. The sensing circuit is relatively complicated and low speed operation is still a problem.

## **2.2 Implemented Direct Back EMF Detection Scheme**

As described in Section 2.1, the noisy motor neutral point causes problems for the sensorless system. The proposed back EMF detection method tries to avoid the neutral point voltage. If a proper Pulse Width Modulation (PWM) strategy is selected, the back EMF voltage referred to  $V_{DC}/2$  signal can be extracted directly from the motor terminal voltage. The special event trigger from the dsp PWM module is used to initiate conversion of the ADC signals just before the switches turn off. The  $V_{BUS}$  voltage is sensed as  $V_{DC}$  using resistor pairs, and  $V_{DC}/2$  signal is used as the zero crossing reference voltage for back EMF sensing. The PWM signals are arranged in complementary mode, due to the duality in the system operation. The PWM signals are applied to both high and low side inverter switches. To implement the complementary PWM algorithm, dead time is necessary to prevent cross conduction between high side and low side MOSFETs in the bridge inverter. The DSP controller has built-in dead time generation to avoid cross conduction. Both center-aligned and edge-aligned PWM signals can be implemented due to flexibility in the DSP software programming. Figure 2.6 shows the concept of detection circuit. The difference between Figure 2.4 and Figure 2.6 is that the motor neutral voltage is not involved in the signal processing as shown in Figure 2.6.

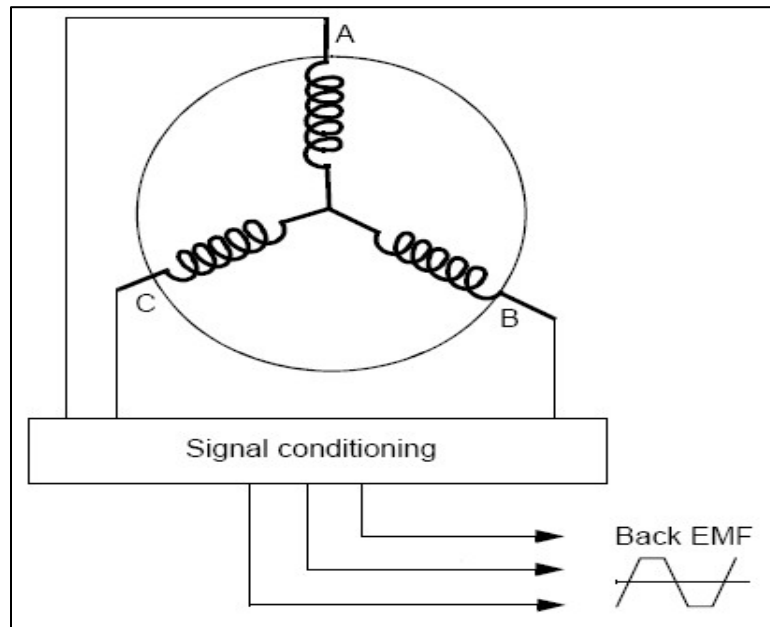


Figure2.6: Proposed back EMF zero crossing detection scheme.

The DSP controller has a high speed A/D converter that is used for this purpose. Using potential divider, the back EMF signal is brought down to a level that the DSP can measure. The signal is sampled by the A/D, and is continuously compared with a digital value corresponding to the zero point. When the two values match, the commutation sequence is updated. The advantage with this method is that it is more flexible in terms of measurement. When the speed varies, the winding characteristics may fluctuate, resulting in variation of back EMF. In such a situation, the DSP has complete control over the determination of zero crossing point. Also, digital filters are implemented to filter out the high frequency switching noise components from the back EMF signal.

The commutation algorithm used is the standard BLDC control algorithm. The commutation occurs 30 electrical degrees after the back EMF zero crossing. Due to easy programmability of the microcontroller, the system has much flexibility to operate the motor